TECHNISCHE UNIVERSITÄT MÜNCHEN
LEHRSTUHL A FÜR THERMODYNAMIK
o. PROF. DR.-ING. F. MAYINGER

ENTRAINMENT AND PHASE SEPARATION IN GAS-LIQUID-MIXTURES

by

F. Mayinger

presented at

Second International Symposium on "gas-liquid flow in pipes 1987"
Mexico, August, 1987

Entrainment and Phase Separation in Gas-Liquid-Mixtures

F. Mayinger

1. Introduction

The characteristics of fluid flow and heat transfer in gas-liquid-mixtures are depending on the distribution of the phases - called flow pattern - and the relative velocity between the phases - known as slip. Flow pattern and slip define the intraction at the phase interfaces and the transport phenomena. There are two special situations of flow behaviour with rather well defined phase intractions. One is present in annular flow pattern with a liquid annulus at the pipe wall and a gas-or vapour core in the center of the flow cross section which, however, is entrained with liquid droplets. The other situation is typical for stagnant or almost stagnant liquid swelled by gas or vapour separating by buoyancy forces.

At a first sight it seems to be rather easy to formulate correlations for describing the flow behaviour in these two situations and for predicting the entrainment in annular flow and the phase separation in gas containing liquid because the flow pattern seem very well defined. Nevertheless, also these flow conditions are difficult enough for a theoretical analysis which is mainly due to the unknown momentum exchange at the phase interfaces and the lack of exact knowledge of the detailed phase distribution.

2. Entrainment

In a rather simplified conception one could assume that in annular flow the total liquid flows in an annulus of smooth or wavy surface at the wall and the gas or vapour moves whithout liquid in the center of the channel. The reality, however, is different from this conception. Only a part of the liquid phase is found as liquid annulus at the wall of the channel or the tube and a not-inconsiderable part of the liquid is carried as droplets - as shown in Fig.1 in the gas core of the flow. This portion of liquid is called entrainment. Usually the droplet mass flow rate M_{ent} in

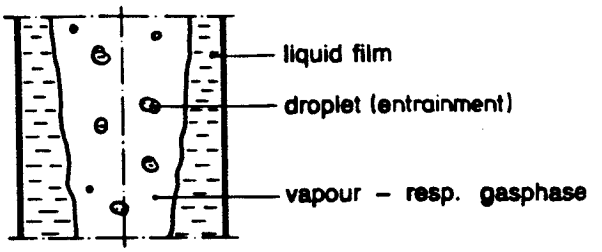

Fig.1: Phasedistribution with annular flow and high vapour quality

the gas core is related to the total liquid mass flow rate $M_{l,tot}$ and one gets then a dimensionless definition for the entrainment E:

$$E = \frac{\dot{M}_{ent}}{\dot{M}_{l,tot}} \tag{1}$$

In the literature the entrainment sometimes is also related to the local instantaneous conditions as it is usual with the local void fraction ε and one gets then the local volume of the entrained mass in comparison to the local volume of the total mass.

$$e = \frac{V_{ent}}{V_{l,tot}} = \frac{A_{ent}}{A_{l,tot}} = \frac{A_{ent}}{A_{tot}(1-\varepsilon)} \tag{2}$$

The latter definition one can also regard as the averaged droplet-cross section to the total cross section covered by liquid.

Looking from the top actually into the gas-liquid-mixture flowing in an annually-like condition one has to realize that the phase distribution in reality is much more irregular and more complicated to be described than we assumed this when we discussed Fig.1.

Fig.2 shows a view in a vertical tube where in the left photograph just annular flow is forming. In the photograph at the right side, which shows the conditions at higher void fraction one realizes that the liquid film at the wall has not an uniform thickness but is wavy distributed over the circumference of the tube wall. For getting an idea of the droplet diameters and the thickness of the liquid film one has to mention that the tube shown in Fig.2 has a diameter of

14 mm. One then realizes that the droplets in the right hand photograph are all smaller than 1 mm and that on the left photograph the liquid is forming filaments like bridges crossing the vapour core. This is a flow condition between churn flow and fully developed annular flow.

Fig.2: Entrainment and distribution of liquid film in a tube /1/

For a better understanding of the phase interface transport phenomena between liquid and vapour we have briefly to discuss how the droplet entrainment in the vapour core arises. As cause for the relief of droplets out of the liquid film the presence of surface waves is considered in the literature usually. The formation of waves at the phase interface originates from instabilities which are caused by the momentum exchange between the phases flowing with different velocities. The velocity of the gas or vapour is higher at the top of the wave than on its ground. The difference in pressure connected with this higher and lower flow velocities causes the amplitudes of the waves to grow until the originally sinusoidal wave detortes in such a way that liquid can be separated by the gas- or vapour flow.

This detorsion can have a form that the gas or vapour flowing with higher velòcity than the liquid can undercut the wave as shown in Fig.3. This undercutting can be explained by the fact that the forces resulting from the shear stresses at the phase interface are acting opposite to the direction of the movement of the wave and are preventing the top of the wave from flowing with the same velocity as the liquid film. Finally a gas- or vapour cushion is forming under the top of the wave which in addition is influenced by the surface tension. By this a liquid membrane or droplet separates and moves into the gas flow.

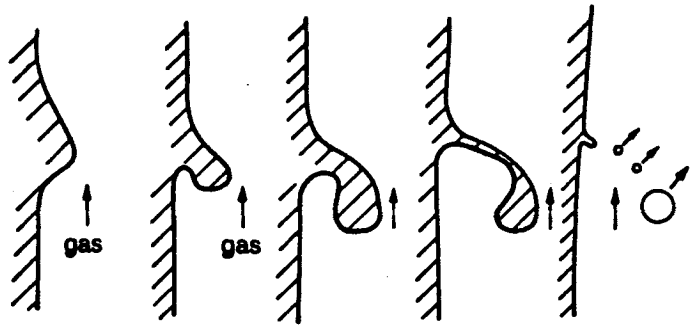

Fig.3: Entrainment formation by "undercutting" of the liquid wave

From observing the sea at the shore we know that waves turn over approaching the shore. The same behaviour can also be observed with gas-liquid mixtures flowing in tubes. The liquid flowing at the wall is influenced by the shear stress from the wall decelerating it. At the phase interface the gas- or vapour flow is accelerating the liquid. By this the top of the waves are forced to move faster than the liquid in the annulus and so - as shown in Fig.4 - droplets or liquid membranes are separated from the surface of the liquid and carried by the gas flow. This phenomenon is mainly observed in thin liquid films.

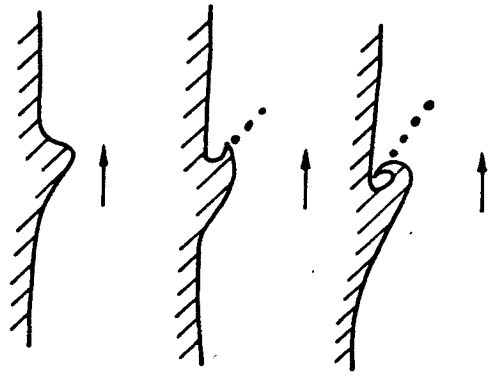

Fig.4: Entrainment formation by "surf" waves

Finally, we have to discuss the formation of entrainment by penetrating of gas or vapour through the liquid film at the wall. This vapour-penetration only occurs if the wall is heated. A bubble which penetrated the liquid film, arrives at the surface, is resting there for a moment, and forms a lentil-like top there. During this resting of the gas bubble at the surface the liquid layer enveloping the bubble

is carried off by the rubbing over gas forming a second smaller top due to surface tension as illustrated in Fig.5 and finally a liquid particle is carried away in form of a lamina. The remaining pit is filled up by the liquid flowing in from the side and the effect of inertia forms a small liquid jet or a droplet contributing to the entrainment too.

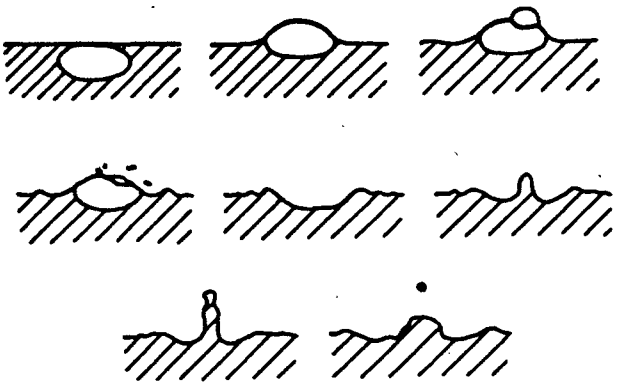

Fig.5: Entrainment formation by gas-bubbles in liquid film

These various mechanisms of entrainment result in different sizes of droplets which spectrum, however, does not cover such a wide field as one could assume from the physical occurances. Langner /1/ demonstrated in his experiments that as shown in Fig.6 even with relatively low velocities of the vapour or gas - for example 3 m/s - hardly droplets are present, of which diameter is larger than 1 mm. With vapour velocities of 9 m/s only 10% of the droplets are larger than 0,25 mm. The measurements by Langner were performed with the refrigerant R12 with a pressure of 9 bar. Wicks and Duckler /2/ investigated water-air-mixtures of ambient pressure and found - however with higher gas velocities - 23 m/s - a droplet-spectrum of much smaller diameters as demonstrated in Fig.6.

The liquid droplets, however, are not only teared away from the liquid at the wall but also carried back to it, which is called de-entrainment. Therfore along the slow path one can imaginate three different regions:

- a first one in which the tearing off out of the liquid film into the gas core prevails
- a second one in which more liquid is lied down to the film than seperated from it and
- a third one in which the entrainment and the de-entrainment are in equilibrium.

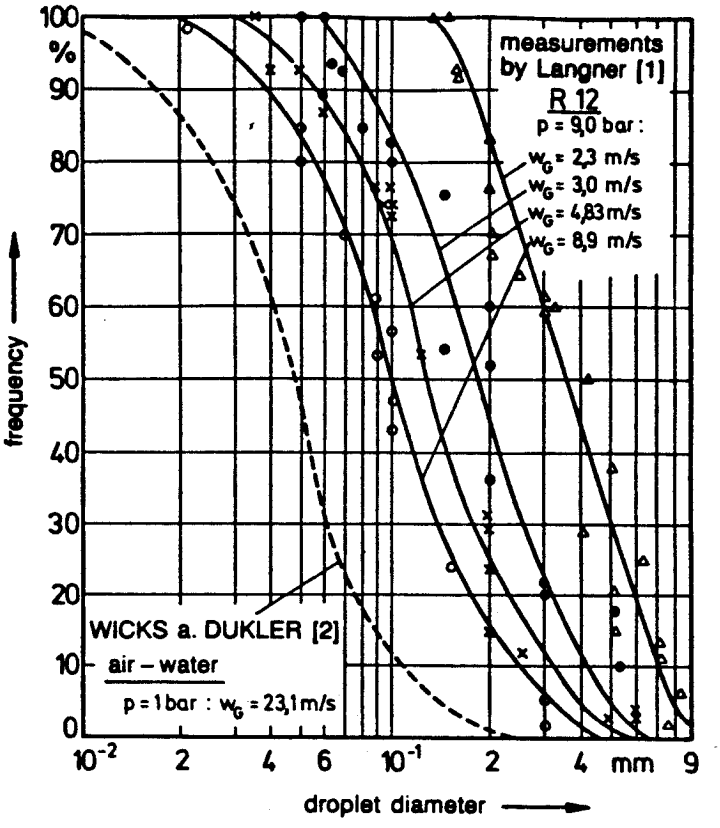

Fig.6: Droplet spectrum in entrainment, heated R12 flow and adiabatic air-water flow

Under the first condition, mentioned above, the liquid mass in the gas- or vapour-core is increasing contineously. This behaviour can be explained by the velocity distribution over the cross section of the vapour core.

With low void fraction velocity profiles are to be expected in the liquid film and in the vapour core as demonstrated in Fig.7. The vapour velocity is due to the low void fraction not too high and because of the large burden with droplets which increases the momentum exchange transverse to the flow direction a flat velocity profile of highly turbulent character is setting in. Due to the small differences of the velocities in radial direction also the radial forces - the de-entrainment forces - onto the droplets are low. On the other hand, however, the liquid film tends to form waves which improves the tearing off of the droplets and, therefore, the entrained mass out of the liquid film is larger than the de-entrained one.

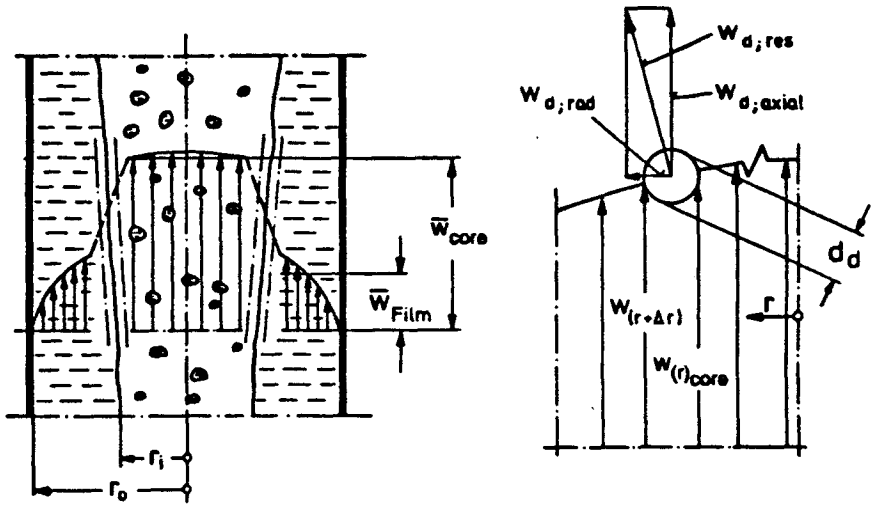

Fig.7: Velocity profile with low void fraction

High void fractions signify thin liquid films tending less to wave formation and so suppressing the tearing off of droplets. The core of the gas has almost a parabolic velocity profile as shown in Fig.8 which imposes to the droplets a higher movement tending in radial outwards direction due to the higher velocity gradient in the vapour core. Under these conditions, therfore, the de-entrainment - the replacing of droptlets to the wall - is prevailing.

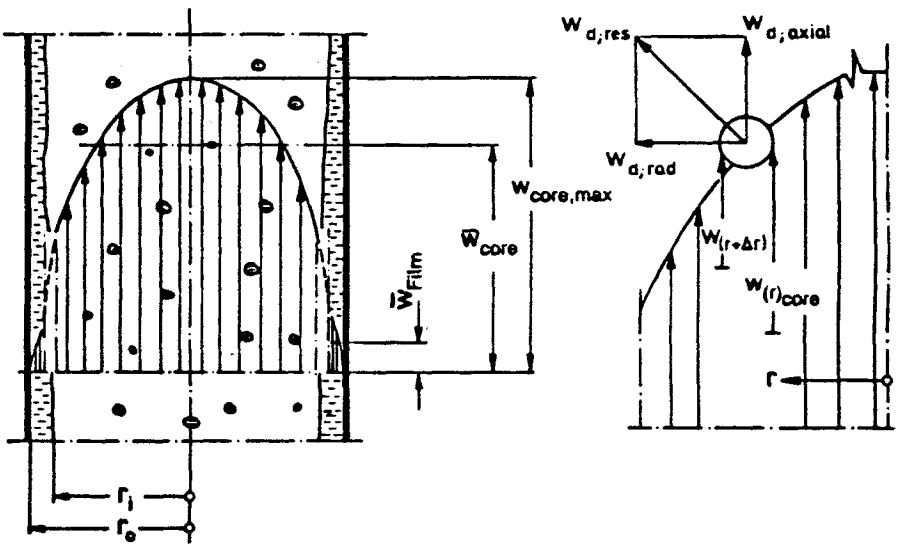

Fig.8: Velocity profile with high void fraction

The radial velocity of the droplets, however, is also depending on the droplet diameter. In Fig.9, presenting an example of a refrigerant-flow of 300 kg/m^{2}s mass flow rate and a quality of x = 0,8 kg/s vapour per kg/s total mass flow

measurements /1/ of the radial velocity of the droplets as a function of the droplet diameter are presented. One realizes that large droplets have a very small tendency to de-entraine and mainly the small droplets are migrating in diagonal direction with less than 1/10th of the axial vapour velocity.

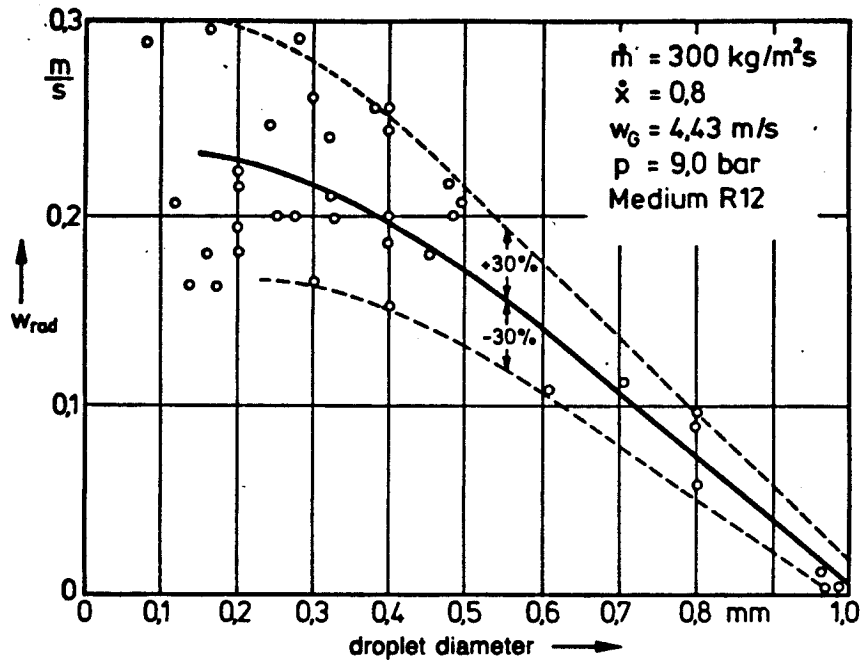

Fig.9: Radial droplet velocity in annular flow

Measurements of the droplet- and liquid-distribution across the flow direction were early reported by Gill /3/. He investigated a water-air-mixture and found as one can see in Fig.10 a distribution of the liquid mass flow in the vapour core having an increasing radial gradient with higher total liquid mass content. The mass flow rate of the air was kept constant in the experiments by Gill. From Fig.10, however, one must not conclude that the local concentration of droplets - in kilogramm locally entrained liquid mass per kilogramm total local liquid mass - is essentially higher in the center of the tube than at the side where the liquid film moves because there the local velocity is much lower than in the center of the tube.

Statements of generalized character can only be made if the entrained mass is in a condition which is called "hydrodynamic equilibrium", i.e. if the same amount of droplets is teared off from the liquid film at the wall as is replaced from the gas core to this liquid film. This needs a long inlet length of the flow and a very careful experimental technique. Such measurements in water-vapour-mixtures are reported

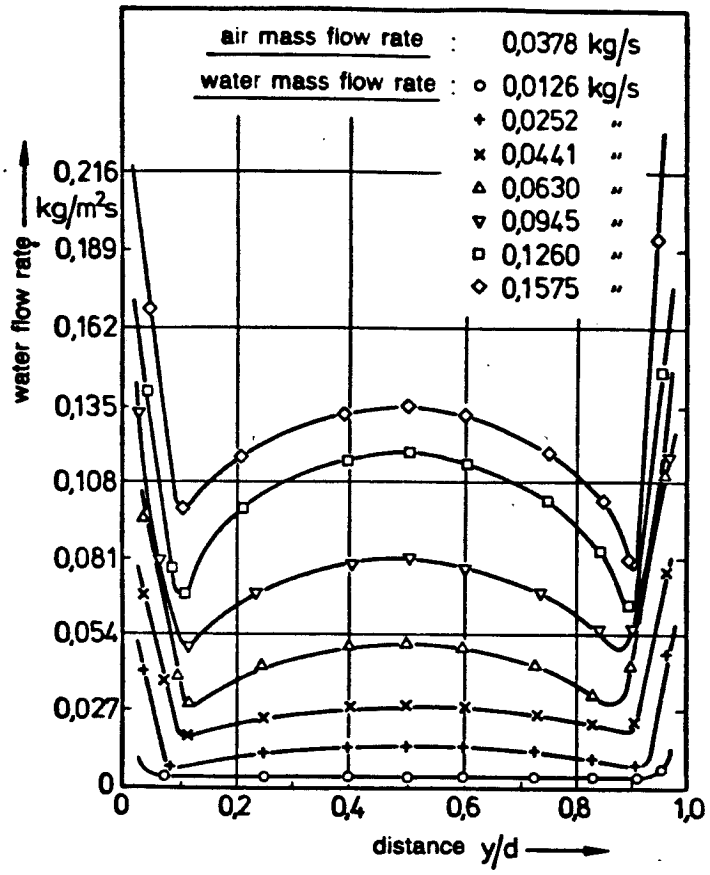

Fig.10: Liquid distribution in an air-water flow acc. Gill /3/

by Bennet /4/. For representing the entrainment behaviour in two-phase flow a plot as shown in Fig.11 became usual in the literature. In such a plot the quality $\dot{x}$ forms the abszissa and the mass flow rate of the liquid carried in the vapour or in the gas - the entrainment - the ordinate. If the wall of the tube would be totally unwetted the mass flow rate of the entrainment versus the quality would follow a straight line which course can be represented by the simple equation

$$\dot{M}_l = \dot{M}_{ent} = (1 - \dot{x})\,\dot{M}_{tot} \tag{3}$$

because all liquid is now flowing in form of the entrainment. In reality there is a liquid film at the wall as long as the shear stress of the vapour flow allows its exsistence. The mass flow rate of the liquid in the film M_f is the difference

$$\dot{M}_{film} = \dot{M}_{tot} - \dot{M}_{ent}$$

of the total liquid mass flow rate M_{tot} and the liquid flow rate entrained in the vapour core M_{ent}. Knowing the entrainment and the vapour velocity or the slip ratio the thickness of the liquid layer at the wall - assuming equal distribution over the circumference - can be calculated. Fig.11 shows that the absolute entrained mass flow rate has a maximum at medium qualities $\dot{x}$. It has to become zero at $\dot{x}$ = 1,0 per definition. This condition has not to be fulfilled at $\dot{x}$ = 0 in any case because with heat fluxes higher than the critical heat flux there does not exist a liquid film at the wall but a vapour film merging the total liquid into the center of the tube.

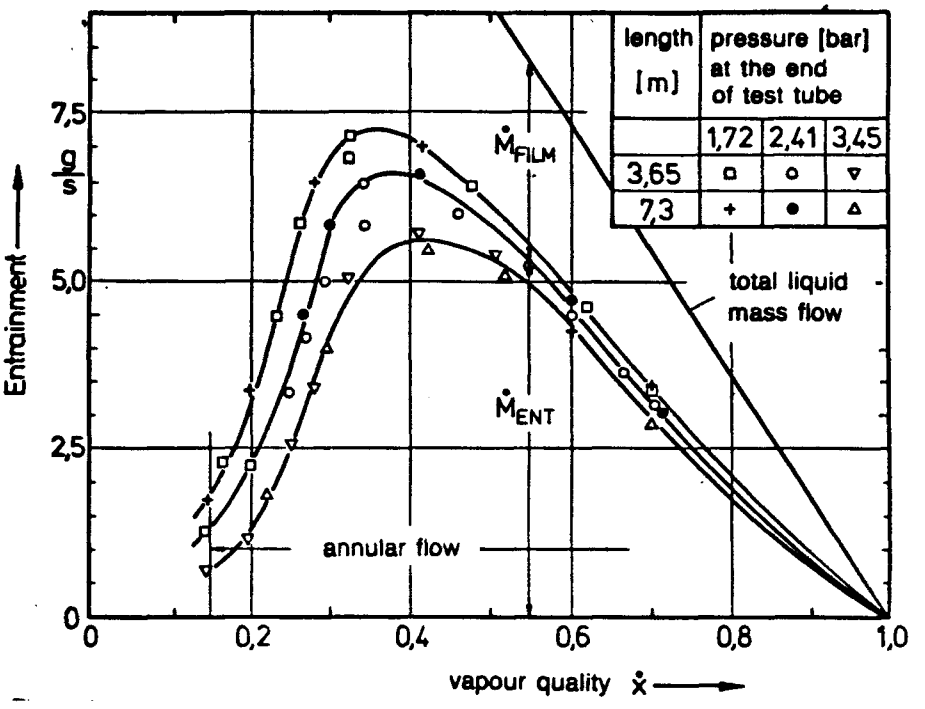

Fig.11: Entrainment with hydrodynamic equilibrium acc. Bennet /4/, water steam mixture d = 12 mm,unheated

The liquid mass carried in the gas or vapour, respectively, is increasing with higher pressure. This can easily be explained with the experimental conditions of the measurements presented in Fig.11. There existed a vapour-water-mixture of saturated conditions which pressure and temperature followed the saturation line. With increasing temperature the surface tension decreases which means that the tearing off of water droplets out of the liquid film at the wall is facilitated. In addition the density of the gaseous phase becomes higher and by this larger momentum forces can be transfered to the liquid layer.

One must not be missled by the maximum in Fig.11 to the opinion that the relative entrainment E, equ.(1), is decreasing again with increasing quality. To get

the true answer we always have to put in relation the total liquid flow rate - straight line in Fig.11 - to the entrained one.

The conditions are different if the wall of the tube is hot. The heat addition from the tube wall to the liquid results in a diminution of the liquid film at the wall by evaporation which supports the tearing off of droplets from the liquid film. Therefore it is easily understandable that with high void fractions, as demonstrated in Fig.12, the entrainment of a heated two-phase flow is higher than that of an adiabatic one. Looking to Fig.12, however, one is surprised that at low void fractions the curve for the entrainment of heated flow is below that of hydrodynamic equilibrium in unheated flow. One, however, has to take in account that the length of the tube used in the heated flow - Fig.12 - was much shorter than needed to reach hydrodynamic equilibrium.

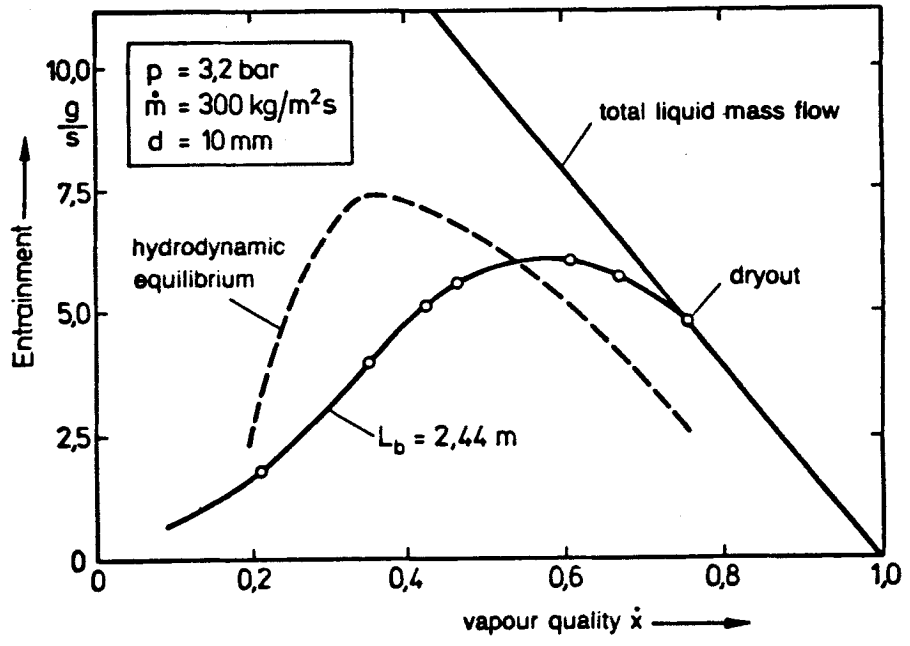

Fig.12: Entrainment in heated flow acc. Bennet /4/

The point where the entrainment curve meets the straight line of total liquid mass flow represents the dryout condition. All liquid is now carried in the vapour core.

The mass flow rate of the two-phase mixture has large influence - as easily understandable - onto the entrainment. High mass flow rates of the mixture carry large amounts of liquid in the gas core as Fig.13 demonstrates and the dryout

occurs with lower qualities. The experimental results shown in Fig.13 were measured in the refrigerent R12 at a pressure of 12,8 bar /1/. Scaled to water with the condition that the density ratio of liquid and vapour in the refrigerant and in the water should be the same this corresponds to a pressure of little more than 80 bar in water.

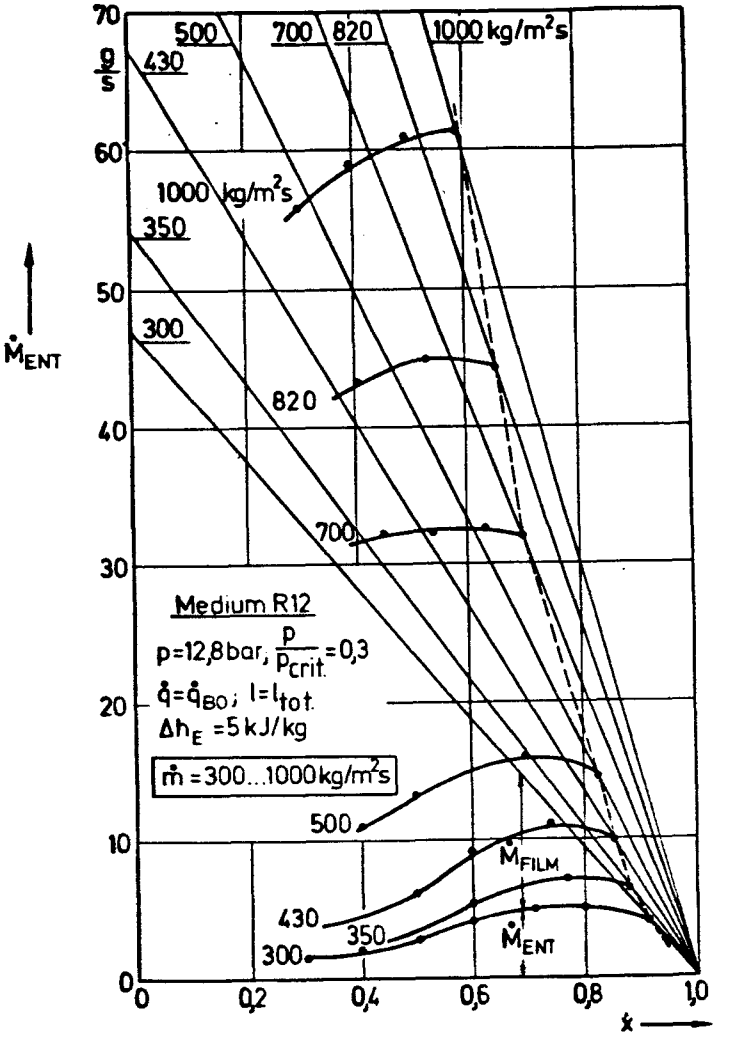

Fig.13: Influence of mass flow rate on entrainment acc. Langner /1/, tube diameter 14 mm

The heat flux density of the tube wall has a negligible influence onto the entrainment and also a variation of the pressure results in a much smaller change of entrainment compared to that what we have seen in Fig.11 at a much lower pressure level. The reason for this is very simple. The vapour or gas has a much higher compressibility at lower pressure than at higher ones and therefore the momentum transfer from the vapour to the liquid changes much stronger with pressure at lower pressure levels than at higher ones. Short pipes show lower

entrainment than long ones. After inlet lengths of 3 - 5 m, however, also this influence is hardly noticeable.

As obvious this graphical description of the physical occurences is as difficult is its theoretical description. Langner /1/ made an attempt to predict theoretically - or better semiempirically - the entrainment of gas-liquid mixtures. He derived the change of the entrainment E versus the tube length - the flow path - from a momentum balance

$$\frac{dE}{dz} = \frac{1}{\dot{M}_{tot}(1-\dot{x})}\frac{d\dot{M}_{ent}}{dz} - \frac{E}{\dot{M}_{tot}(1-\dot{x})}\left[(1-\dot{x})\frac{d\dot{M}_{tot}}{dz} - \dot{M}_{tot}\frac{d\dot{x}}{dz}\right] \tag{4}$$

Equ.(4) simply results by differentiating equ.(1) taking in account that for transient conditions the total mass flow rate M_{tot} versus the axis z of the tube is not constant. The total mass flow rate M_{tot} is the sum of the vapour mass flow rate and the total liquid mass flow rate, the latter one resulting again from the entrained liquid and the liquid flowing at the wall. Equ.(4) can be re-arranged in that way that the change of the entrained mass flow rate versus the axis z of the tube is the independend variable.

$$\frac{d\dot{M}_{ent}}{dz} = \dot{M}_{tot}(1-\dot{x})\left[\frac{dE}{dz} + E\left(\frac{1}{\dot{M}_{tot}}\frac{d\dot{M}_{tot}}{dz} - \frac{1}{1-\dot{x}}\frac{d\dot{x}}{dz}\right)\right] \tag{4a}$$

For steady-state conditions equs.(4 and 4a) can be simplified into the form

$$\left.\frac{dE}{dz}\right|_{stead} = \frac{1}{\dot{M}_{tot}(1-\dot{x})}\frac{d\dot{M}_{tot}}{dz} + \frac{E}{1-\dot{x}}\frac{d\dot{x}}{dz} \tag{4b}$$

respectively

$$\left.\frac{d\dot{M}_{ent}}{dz}\right|_{stead} = \dot{M}_{tot}\left[(1-\dot{x})\frac{dE}{dz} - E\frac{d\dot{x}}{dz}\right] \tag{4c}$$

We have now to develope a momentum balance to calculate the entrainment. It seemed to be advisible and in some respect benificial to position the border for this momentum balance to the phase interface between vapour-core and liquid film at the wall because the forces there are relevant for the liquid exchange and by this

for the entrainment. The volume which has to be demarcated for the momentum balance, therefore, is surrounded by the surface area of the gas-core in the flow $\int 2 \cdot \pi \cdot r \, dr$ and the step dz of the integration. Formulating the momentum balance of the mixture in the gas- or vapour-core of the flow one has to take in account the pressure drop acting along the channel length, the gravitation force, and the friction at the border between gas-core and liquid film resulting from the shear stress. The terms of the momentum balance and the balance border are illustrated in Fig.14. Under transient conditions also the variation of the momentum fluxes

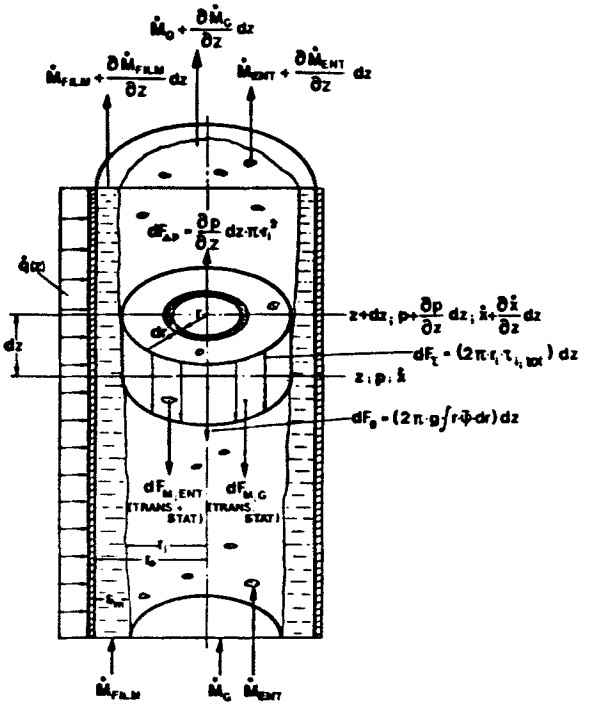

Fig.14: Momentum balance for entrainment calculation

with time has to be regarded. Balancing of momentum fluxes and forces result in the general equation

$$\frac{\delta}{\delta x}\left(\dot{m}_g w_g + \dot{m}_{ent} w_{ent}\right) \iiint_V dV + \frac{\delta}{\delta t}\left(\dot{m}_g + \dot{m}_{ent}\right) \iiint_V dV =$$

$$\left[p - \left(p + \frac{\delta p}{\delta z} dz\right)\right] \iint dA_q - \pi_i \iint dA_{filmsurface} - g\bar{\rho} \iiint_V dV \qquad (5)$$

For a channel with constant cross section along the axis z equ.(5) can be written in a simplified form:

$$\frac{\delta}{dz}\left(\dot{m}_g w_g + \dot{m}_{ent} w_{ent}\right) dz \iint dA_q + \frac{\delta}{\delta t}\left(\dot{m}_g + \dot{m}_{ent}\right) dz \iint dA_q =$$
$$\left[p - \left(p + \frac{\delta p}{\delta z}\right)\right] \iint dA_q - \pi_i \iint dA_{filmsurface} - g\bar{\rho} dz \iint dA_q \qquad (5a)$$

Finally one can write equ.(5a) for a channel of cylindrical cross section which will be treated in the following derivations only.

$$\frac{\delta}{\delta z}\left(\dot{m}_g w_g + \dot{m}_{ent} w_{ent}\right) dz \int_0^{r_i} 2\pi r dr + \frac{\delta}{\delta t}\left(\dot{m}_g + \dot{m}_{ent}\right) dz \int_0^{r_i} 2\pi r dr =$$
$$\left[p - \left(p + \frac{\delta p}{\delta z} dz\right)\right] \pi r_i^2 - 2\pi r_i dz \tau_i - g dz \int_0^{r_i} 2\pi r \bar{\rho} dr \qquad (5b)$$

The equs.(5a-b) contain on their left side

- the difference between inlet and outlet momentum flux of the fluid
- the stored or destored momentum in the balance volume

and on their right side

- the pressure drop along the channel length
- the retarding force from the dissipated energy and
- the buoyancy force.

The equs.(5a-b) cannot be integrated in the form as shown above, also not in a numerical way because additional informations on the fluiddynamic behaviour of both phases are needed. Starting on the left side of the equations we at first are faced with the question concerning the velocity w_g of the vapour and the velocity w_{ent} of the droplets contained therein. The velocity of the vapour or gas we can derive from the slip correlations known in the literature, however, we do not know how the velocity of the droplets is different from that of the vapour. At the beginning of this chapter we learned that the droplets are very small and their diameter hardly exceeds 1 mm which means that they flow probably unessential slower than the vapour. Using the droplet spectrum he measured and by estimating the relative velocity between the droplets and the vapour Langner /1/ could prove that, neglecting the difference in the velocities of the droplets, the vapour has less than 1% influence onto the result of the entrainment calculation. Therefore, one can impute that the vapour and the droplets flow with the same velocity at each distinct radial position of the cross section of the tube. With this assumption we

can write

$$w_{ent} = w_g = \dot{m}_{tot} \left(\frac{r_0}{r_i}\right)^2 \left[\frac{\dot{x}}{\rho_g} + E\frac{(1-\dot{x})}{\rho_f}\right]$$

which enables us now to calculate the velocity of the mixture in the gas-core.

Furthermore we can assume that the droplets in the vapour do not evaporate due to flashing by pressure drop because the pressure gradient is small. Finally, we assume that the droplets are homogeneously distributed over the cross section of the vapour-core and that this radial distribution is not changed along the pipe axis dz. The homogeneous distribution of the droplets across the gas-core was proved by the measurements of Adorni /5/. This assumption allows to describe the term of the gravity forces in the equs.(5a.b) as the sum of the weight of the separate phases. With these assumptions and simplifications one finally can write the momentum balance in the form:

$$\begin{aligned}
&\pi r_i^2 \frac{\delta}{\delta z}\left[\dot{m}_{tot}^2 \left(\frac{r_0}{r_i}\right)^2 \left[\frac{\dot{x}}{\rho_g} + \frac{E(1-\dot{x})}{\rho_l}\right][\dot{x} + E(1-\dot{x})]\right] dz + \\
&\pi r_i^2 \left[\dot{m}_{tot}(1-E)\frac{\delta \dot{x}}{\delta t} + \dot{m}_{tot}(1-\dot{x})\frac{\delta E}{\delta t} + (\dot{x} + E(1-\dot{x}))\frac{\delta \dot{m}_{tot}}{\delta t}\right] dz = \\
&\pi r_i^2 \left[p - \left(p + \frac{\delta p}{\delta z} dz\right)\right] - 2\pi r_i \tau_i dz - \pi r_i^2 g\left(\rho_l(1-\varepsilon_{core}) + \rho_g \varepsilon_{core}\right) dz
\end{aligned} \tag{6}$$

For the numerical solution of this differential equations the boundary conditions and the shear stress τ_i between the liquid film and the gas-core have to be known. For the boundary conditions the temporal and local borders have to be taken in account. If, for simplicity case, we at first assume steady-state flow, than the temporal boundary condition can be omitted and - for example - in describing the flow inside the pipe of a steam generator we can assume that the position of the dryout in the pipe is known from burnout-equations of the literature. With such a burnout-equation the axial position where the entrainment is unit, E = 1, is known. From this dryout position one then has to integrate backwards, i.e. upwards of the flow. In cases where no dryout occurs in the tube the integration of the entrainment has to start at the exit or at the inlet of the tube, where the

entrainment has to be known. One also can try to start from the position where boiling starts, then however, one needs informations on the formation of the flow pattern, especially the voidage distribution at the position where churn flow changes in annular flow.

In the following we will consider steady-state flow only. For transient behaviour and especially for the derivation of the entrainment-equations in detail it is referred to the Ph.D-thesis by Langner /1/ . For steady-state flow the mass flow rate density is independent from the flow path. Assuming in addition that entrainment calculations are only of interest for small thickness of the liquid film at the wall, one can set the ratio between the radius of the tube and the inner radius of the liquid film unit, $r_o/r_i = 1$, in a first approximation. By this we get

$$\frac{d}{dz}\left(\frac{r_o}{r_i}\right)^2 = 0$$

With this simplification equ.(6) can be written in the form:

$$\frac{dE}{dz} = -\left[\frac{\frac{2\tau_i}{r_i} - \frac{dp}{dz} + \frac{\dot{x}+E(1-\dot{x})}{\dot{x}+E(1-\dot{x})\rho_g/\rho_l}\rho_g g}{\dot{m}_{tot}^2\left(\frac{r_o}{r_i}\right)^4\left[\left(\frac{1-\dot{x}}{\rho_l}\right)(\dot{x}+E(1-\dot{x}))+\left(\frac{\dot{x}}{\rho_g}+\frac{E(1-\dot{x})}{\rho_l}\right)(1-\dot{x})\right]} + \frac{T_1}{T_2}\frac{d\dot{x}}{dz}\right] \qquad (6a)$$

$$T_1 = (\dot{x}+E(1-\dot{x}))\left(\frac{1}{\rho_g}-\frac{E}{\rho_l}\right)+\left(\frac{\dot{x}}{\rho_g}+\frac{E(1-\dot{x})}{\rho_l}\right)(1-E)$$

$$T_2 = (\dot{x}+E(1-\dot{x}))\left(\frac{1-\dot{x}}{\rho_g}\right)+\left(\frac{\dot{x}}{\rho_g}+\frac{E(1-\dot{x})}{\rho_l}\right)(1-\dot{x})$$

To solve equ.(6a) we need correlations for the shear stress τ_i at the border between the gas-core and the liquid film and for the friction pressure loss dp/dz along the flow path. In a steady-state flow without acceleration this friction pressure loss is equal to the pressure drop. For calculating the friction pressure loss we can use correlations known from the literature. Langner /1/ used in his thesis the correlation by Baroczy-Chisholm /6/ which showed good agreement with measurements in the refrigerant R12. However, one can also use other correlations like the correlation by Friedel /7/.

Studying the literature we find also correlations describing the shear stress between the gas-core and the liquid film at the wall. One, for example, was presented by Ishii /8/ written in the form:

$$\tau_i = 0,005 \left(1 + 300\frac{\delta}{D_0}\right) \rho_g \frac{(w_g - w_{l,film})^2}{2} \tag{7}$$

Ishii developed his correlation by using experimental results measured in adiabatic flow with air-water mixtures. This correlation can also be used for evaporating two-phase flow if very high void fraction exists and the liquid film at the wall is thin and not too wavy on its surface. Another correlation was presented by Ueda and Nose /9/ who assumed in their derivation that the momentum tranfer between between the gas-core and the liquid film can be described as the sum of the shear stresses of the pure gas on the liquid and the momentum exchange by de-entrained and entrained droplets.

Langner /1/ found in his investigations that the correlation by Levy /10/ is quite useful for describing entrainment behaviour because it gave good agreement with his entrainment experiments. The correlation by Levy /10/ is based on the assumption that the stear stress at the border between gas-core and liquid film consists of two terms

- one friction term due to the velocity difference between gas-core and liquid film and
- one momentum term due to droplet entrainment and de-entrainment at the surface of the liquid film.

Levy uses the well-known turbulence-models known in single-phase flow and introduces a local oscillatory component of the density and of the velocity in the direction of the fluid flow as well as an oscillatory component of the velocity perpendicular to the fluid flow. For these oscillatory components he needs a mixing length l for which he uses the Prandtl mixing length theory. Finally, Levy assumes a linear profile of the velocity near the phase interface of the liquid film.

For details on Levy's theory it is referred to the literature /10/. Only the result of the theory by Levy is here of interest for the entrainment calculation. After various simplifications Levy developed two different correlations for the shear stress at the phase interface, one for the case if the friction and the other

one if the gravity of the liquid governs the pressure drop along the channel.

$$\tau_i = \left(\frac{F(0)}{F(1)}\right)^2 \bar{w}\,(\bar{w} - w_{film})\,(\rho_l - \rho_{core}) \qquad for \frac{dp}{dz} \geq g\rho_l \tag{8}$$

$$\tau_i = \left(\frac{F(0)}{F(1)F(2)}\right)^2 \bar{w}\,(\bar{w} - w_{film})\,(\rho_l - \rho_{core}) \qquad for \frac{dp}{dz} < g\rho_l \tag{9}$$

In the equs.(8) and (9) the symbols have the following meaning:

$\overline{w}$ the averaged velocity of the gas-core

ρ_{core} the averaged density of the gas-core and

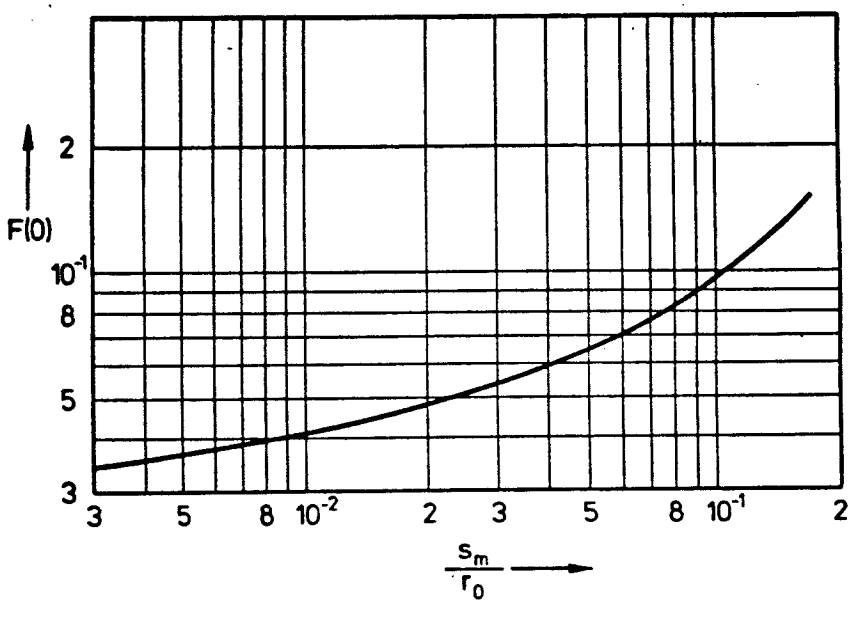

Fig.15: Factor F(0) in equation (8) and (9) acc. Levy, correction for liquid film thickness

The equations contain in addition the empirical correcting factors F(0), F(1), and F(2). The correction factor F(0) is used to take in account phenomena in the liquid film and is only a function of the distance from the wall as long as the mixing length-theory according to Prandtl like in single-phase flow can be used. Its value is plotted in Fig.15 as a function of the distance s_m from the wall in the

liquid film. The correction factor F(1) represents a density correction as shown in Fig.16.

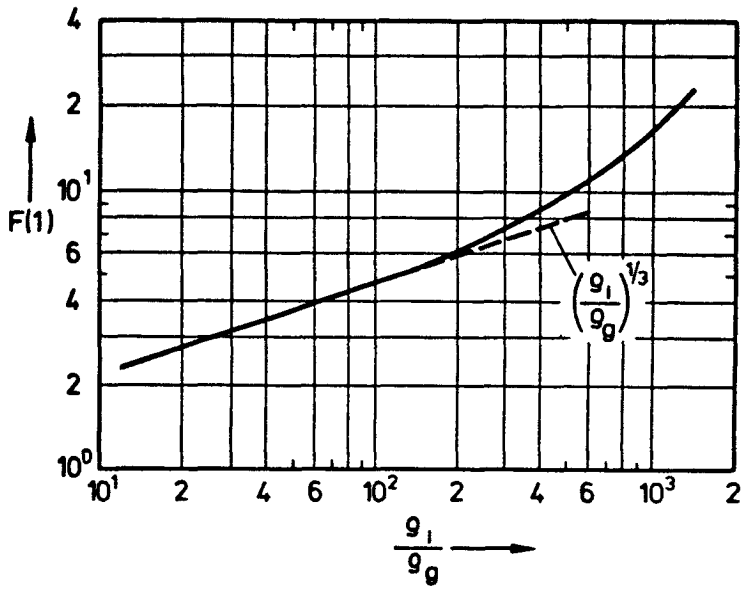

Fig.16: Factor F(1) in equation (8) and (9), correction for density ratio

In case that the force resulting from the pressure drop along the axis of the tube is larger than the gravity force there is the possibility that the liquid film at the wall absorbs more shear force than it is transfered at the phase interface. Therefore, only small surface waves are to be expected at the liquid film and the mixing length theory by Prandtl is well-usable and fully taken in account by the correction factor F(0). However, if the gravity force is larger than the pressure drop along the channel large surface waves can originate. This results in an extension of the mixing length which is expressed in the correction factor F(2)

$$F(2) = \left(\frac{g\rho_l}{-dp/dz}\right)^{-\frac{1}{3}}$$

It was mentioned above that the entrainment behaviour can be organized in two regions, one where the tearing off from the liquid film and the other one where the de-entrainment prevails. These two areas shall be explained again using Fig.17. In the upper diagram shown there, the decrease of the liquid film at the wall is plotted versus the vapour quality $\dot{x}$ and the lower diagram represents the droplet mass flux in the vapour-core also as a function of the vapour quality $\dot{x}$ because the

liquid on its way through the pipe is evaporating. The change of the vapour quality x is also a measure for the distance flown by the gas-liquid-mixture in the tube. The abszissa therefore can also be regarded as a coordinate of the flow path along the tube, however with distorted scale. In the upper diagram of Fig.17 the measured as well as the calculated values bei Langner /1/ are plotted. If the decrease of the liquid film would be only caused by the evaporation due to heat addition, it would be constant following the equation

$$\left(\frac{d\dot{M}_{film}}{dz}\right)_{\dot{Q}_{ad}} = const.$$

because the tube had constant heat flux versus its length. The heat flux was in such a way adjusted that at the end of the 5 m long tube dryout occured.

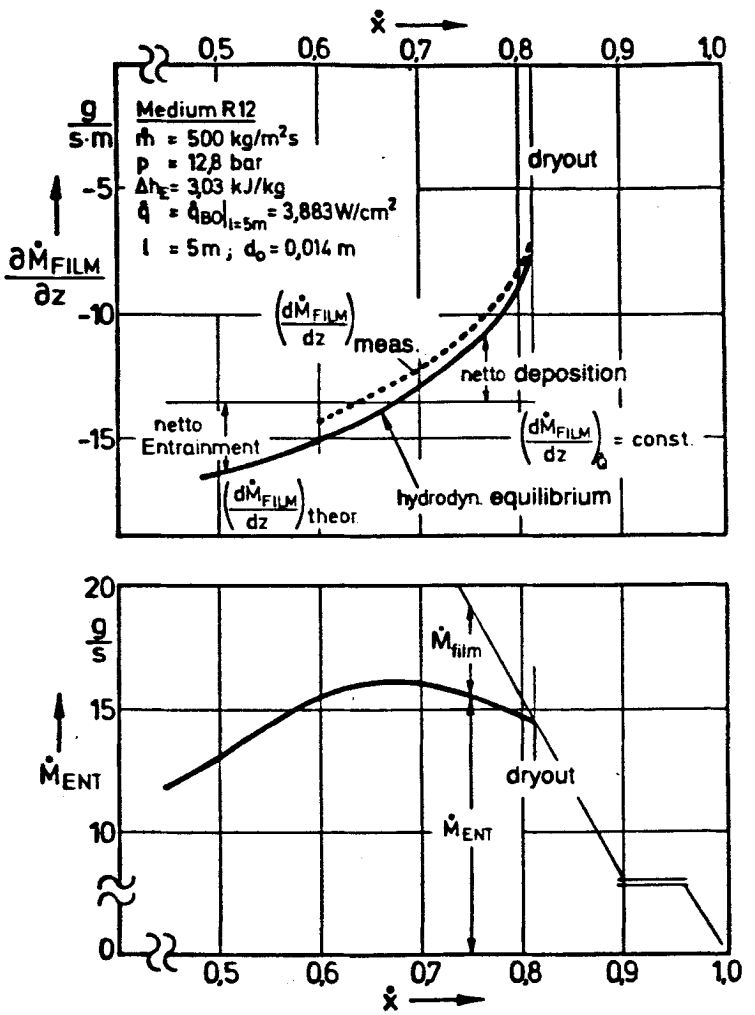

Fig.17: Explanation of entrainment ranges

With small vapour qualities, i.e. in the lower part of the tube, the decrease of the film thickness is larger than it would result from the evaporation. This means

that in addition liquid particles are teared off from the film, what gives the hint that the phenomena in this region are governed by entrainment. With high vapour qualities the decrease of the liquid film is smaller than it would result from the evaporation. This means that here the evaporation is partially compensated by de-entrainment. We can now define a point of hydrodynamic equilibrium at that position where in this heated flow the real entrainment curve intersects with the horizontal line of constant mass evaporated. If we compare this point with the corresponding one in the lower diagram of Fig.17 we realize that it coincides with the maximum of the entrainment curve there.

There are numerous publications on entrainment, droplet sizes, dynamics, and deposition in annular flow also published more recently. It is not possible to discuss them all here in detail and therefore the first aim of this paper was to present a closed theory of possible entrainment discription in two-phase flow which was done above. However, two papers or reports should be mentioned here because of their originality. One is the paper by Lopes and Dukler /11/ and the other one was published by Asali, Leman and Hanratty /10/. In these papers also a very detailed literature survey can be found.

Lopes and Dukler /11/ developed a new laser optics technique that permitted the simultaneous measurement of droplet size and two velocity components in annular flow. The main attributes of the technique are: high precision in the variables measured, high rates of data acquisition making possible a reliable statistical analysis of the data, and small measuring volumes allowing localized measurements and study of radial profiles. So it was possible to develope new insights into the dynamics of the droplet motion and the droplet film interaction. Lopes and Dukler made the following relevant observations:

- The droplets in annular flow cover a wide spectrum of sizes (100-3000 μ m) with a typical average sizes varying around 500 μ m. The size distributions are strongly dependent on gas rates as already stated by Langner.
- Measurements of the axial drop velocity indicated the presence of a considerable slip between gas and droplets. This is in contrast to Langner's assumption. The drop size is such that the droplet dynamics is controlled by particle inertia. Larger droplets travel faster than smaller ones.
- The simultaneous measurement of two velocity components permitted the determination of the distribution of the angle of the velocity vector with the

column axis. Lopes and Dukler showed that these distributions can be used to estimate droplet mass transfer coefficients.

- An analysis of the maximum droplet size revealed that the maximum stable droplet size in annular flow is controlled by the action of forces resulting from pressure fluctuation of the turbulent flow of the gas around the droplet. The critical Weber- number found, based on this criteria, was 0.19.
- The observed independence of radial velocity distributions, with radial position, confirmed that the radial droplet velocity is controlled by the formation process from the liquid film and maintained practically constant along the axial flight.

The authors developed droplet dynamics equations and showed that the velocity predictions from these equations depend strongly on the type of drag coefficient curves used. In a turbulent core the droplet drag coefficient depends not only on the particle Reynolds-number but also on the relative turbulence intensity. The authors used the information they obtained on droplet velocities and rates of entrainment to formulate a momentum balance including droplet exchange. They proposed for future work to measure droplet drag coefficience more in detail because droplet dynamics modelling can be refined only when drag curves are available. Another important problem is according to Lopes and Dukler, the one concerned with the gas velocity profiles and levels of turbulence in the presence of droplets.

Asali et al. /12/ presented new measurements of entrainment for annular flow of air and water-glycerine solutions in pipes. They give clear information about the influence of liquid viscosity onto the entrainment and developed an equation for the entrainment which interprets it as resulting from a balance between the rate of atomization of the wall film and the rate of deposition of droplets entrained in the gas. This atomization-deposition theory gives the entrained mass flow rate as a function of a modified Weber-number (containing the film thickness, a shear stress at the interface, and the surface tension), of the densities and of the gaseous flow rate. Based on the measurements the authors present an empirical fit to presently available entrainment results for high surface tension fluids. This empirical fit represents the measured data well, however, it needs a large number of input variables described by the authors again in empirical correlations so that it would take too much room to present this method here. Reference is made to the original paper /12/.

The most recent paper on droplet entrainment in vertical annular flow - published September 1986 - was written by Lopes and Dukler /13/ too. They correlate the liquid mass carried in the gaseous core as a function of the gas-Reynolds-number and of the liquid-Reynolds-number. Also the pressure drop due to entrainment is correlated in this way.

3. Phase separation

For the construction of components and apparatus in chemical plants and power stations, like steam generators, bubble columns or destillations columns, in which a two-phase vapour-liquid-mixture is present with free surface, frequently data for predicting the upper level of the mixture in the vessel - for the so-called swell level - are needed. In simplified ideas homogeneous distribution of the vapour-or gas-phase and the liquid are assumed or in some cases it is supposed that an entire separation of both phases with forming two layers - the vapour above the pure liquid - takes place. Both assumptions are borderline cases of the real behaviour in which the vapour separation is controlled by the hydrodynamics of both phases in the mixture. The rising vapour- or gas-bubbles have a lifting action on the liquid which then near the wall as outlined in Fig.18 flows downward again

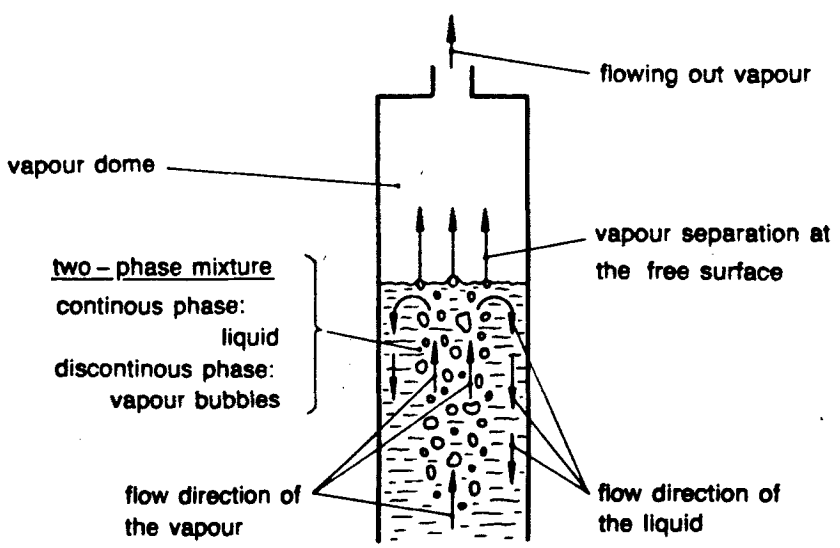

Fig.18: Vapour or gas separation in two-phase mixture

because there are almost no bubbles due to the influence of the wall friction. The rising velocity of the vapour-bubbles in the liquid is controlled by the buoyancy and the drag which the bubble is affected to, when penetrating the liquid. This drag or flow resistance is again depending on the viscosity of the liquid and the size of the vapour bubbles for which the surface tension is a measure for.

It seems to be obvious to start from the movement behaviour of a single bubble for calculating the phase separation and then to introduce empirical corrections for the interaction between the bubbles. By this one could end up with a correlation which predicts the swell level or the void fraction ε averaged versus the hight and the cross section of the vessel or the channel. Correlations derived from these deliberations, however, showed only moderate success. In the literature /14-20/ therefore the dimensionless analysis and a power law were used to describe the averaged volumetric void fraction with phase separation. A selection of such correlations is presented in tab.1. These correlations mostly have the following dimensionless numbers in common:

Froude-number

$$F_r = \frac{w_{g,0}^2}{g\sqrt{\frac{\sigma}{g(\rho_l - \rho_g)}}}$$

Weber-number

$$W_e = \frac{\sqrt{\frac{\sigma}{g(\rho_l - \rho_g)}}}{d_{ves}}$$

and the

Bond-number

$$B_0 = g d_{ves}^2 \left(\frac{\rho_l - \rho_g}{\sigma} \right)$$

The Weber-number is, as well known, the ratio of surface energy forming a bubble or a droplet to the shear forces representing the kinetic energy of the flow which, in this case, is defined by the rising velocity of a single bubble in the vessel. For making easier its application the empirical correlations presented in tab.1 were all refered to a velocity $w_{g,o}$ which would appear if only the gaseous phase would be present in the liquid. Using this "empty-vessel-velocity" has the advantage that with the simple equation

$$w_{g,0} = (\bar{\varepsilon})(\bar{w}_{bub}) \tag{10}$$

the bubble rising velocity $w_{bub.}$ can be derived, knowing the cross section A and the hight H of the vessel.

A comparison of results calculated with the formulas given in tab.1 with measured data under various pressures and with various fluids shows only limited agreement. Viecenz /21/ analysed the different variables influencing the phase separation and found that the viscosity in most of these available equations was not or not correctly taken in account. Based on the correlations in the literature /14-20/ he got the empirical correlation

$$(\bar{\varepsilon}) = C \left[\frac{w_{g,0}^2}{g\sqrt{\frac{\sigma}{g(\rho_l-\rho_g)}}}\right]^n \left[\frac{\sqrt{\frac{\sigma}{g(\rho_l-\rho_g)}}}{d_{ves}}\right]^{0,174} \left[\frac{\rho_l}{\rho_l-\rho_g}\right]^{-0,585} \left[\frac{\nu_l}{\nu_g}\right]^{0,256} \tag{11}$$

for the averaged volumetric void fraction in the vessel. This correlation contains the above mentioned dimensionless numbers, Froude- and Weber-number as well as the ratio of the density ϱ and kinematic viscosity ν of the phases. The Froude-number is afflicted with a constant C and an exponent n in equ.(12) which allow to describe the behaviour of the phase separation with bubbly- as well as with churn-flow. For bubbly-flow, i.e. for values of Froude-number

$$F_r = \frac{\omega_{g,0}^2}{g\sqrt{\frac{\sigma}{g(\rho_l-\rho_g)}}} \leq 3$$

is

$$C = 0,73$$
$$n = 0,376$$

and for churn-flow

$$F_r > 3$$

is

$$C = 0,86$$
$$n = 0,293$$

Equ.(12) allows to reproduce the measured data in the literature within an uncertainty range of ±15%. With bubble- and destillation-columns the liquid fraction in the vessel - which is $1-\varepsilon$ - usually is called hold-up. The usually small cross- and down-flow being present there can mostly be neglected so that equ.(12) is valid there too, presupposed that the hight of the liquid layer is large enough and that inlet- or acceleration-effects with the bubble formation at the holes have a negligible influence onto the phase separation.

The volume of vapour separating per unit of time out of the two-phase flow mixture is sometimes called mean separation velocity $\bar{w}_{sep}$ because of its dimension m/s. This separation velocity is a function of the drift velocity w_{drift}, of the averaged volumetric void fraction as described in equ.(12), of the radial distribution parameter similarly defined as in Zuber and Findlay's /22/ work, and in cases of transient conditions, for example with flashing of the moving velocity w_{surf} of the surface due to flashing.

$$\bar{w}_{sep} = \frac{w_{g,0} C_{0rad}(\bar{\varepsilon})}{1 - C_{0rad}(\bar{\varepsilon})} + \frac{w_{drift}(\bar{\varepsilon})}{1 - C_{0rad}(\bar{\varepsilon})} - w_{surf.}(\bar{\varepsilon}) \tag{12}$$

Viecenz /21/ found the correlation for the drift velocity

$$w_{drift} = 0,2591 \left[\frac{g\sigma(\rho_l - \rho_g)}{\rho_g^2}\right]^{\frac{1}{4}} \left[\frac{\rho_g}{\rho_l - \rho_g}\right]^{0,4755} \cdot \left[\frac{g\frac{\sigma}{(\rho_l - \rho_g)}}{d_{ves}}\right]^{-0,3064} \left[\frac{\nu_l}{\nu_g}\right]^{-0,3405} \left[\frac{H_l}{\sqrt{\frac{\sigma}{g(\rho_l - \rho_g)}}}\right]^{0,0778} \tag{13}$$

In equ.(14) the following formula should be used for the radial distribution parameter $C_{0,rad}$

$$C_{0rad} = C[(\varepsilon)]^a \left[\frac{\rho_g}{\rho_l - \rho_g}\right]^b \tag{14}$$

In equ.(14) H_L stands for the hight of the liquid in the vessel. The constants and exponents in equ.(15) are depending on the mean volumetric void fraction as Viecenz found in his experiments. Values for these constants and exponents in equ.(15) as given by Viecenz are listed in tab. 2.

In equ.(13) w_{surf} becomes zero under steady-state conditions, i.e. if there is no flashing in the vessel. In case of flashing it is very difficult to solve equ.(13)

because one needs information about bubble formation and boiling delay during depressurization to be able to describe the void production and by this the velocity of the surface w_{surf}. A method to perform these calculations is given in /21/.

4. Concluding remarks

Entrainment and phase separation mark two entirely different phenomena in two-phase flow behaviour, however, they have one common feature which is, that the controlling physical processes like the momentum interaction between the phases and the phase interface shear are almost unknown. Therefore, in the literature mostly empirical correlations are used to describe both situations. To get a better understanding of this problem we need experience where for entrainment the droplet drag coefficients within a wide range of turbulence levels, the gas velocity profile, and the frequency modes of oscillation of a viscous droplet are measured. For a complete understanding of annular flow we need a combined analysis of both the contineuous and the dispersed phases. In addition the study of the wave structure of the liquid film is important.

For phase separation in stagnant or almost stangnant liquid we need informations about the circulating flow of the liquid due to the lifting forces of the bubbles, and we have carefully to investigate the drag coefficient around the bubbles and their oscillatory behaviour during rising in the mixture. This also has to be done for a wide range of density and viscosity and for various void fractions. Phase separation in pipes with diameters much smaller than that of vessels is also influenced by wall effects. There are almost no or very rare investigations about phase separation in horizontal pipes with low liquid velocities. Here we have to use correlations predicting the flow pattern, as for example given by Mandhane /23/ or by Taitel and Dukler /24/. They presented correlations with which the different flow regimes can be separated and by calculating the borders between bubbly-, wavy-,churn- and stratified-flow one can draw qualitative conclusions about the void in the upper and lower part of an horizontal tube and by this about the phase separation.

Munich, 30.04.1987
M/Gü

References

/1/ Langner, H., Untersuchungen des Entrainment-Verhaltens in stationären und transienten zweiphasigen Ringströmungen. Dissertation, Technische Universität Hannover, 1978.

/2/ Wicks, M., Dukler, A.E., Measurements of drop-size distribution in two-phase flow, Intern. Heat-Transfer-Conference, Chicago, 1966.

/3/ Gill, L.E., Hewitt, G.F., Lacey, P.M.C., Sampling probe studies of the gas-core in annular two-phase flow, Part 2. Chem.Engng. Sci. 19, 665 (1964).

/4/ Bennet, A.W., Hewitt, G.F., Kearsey, H.A., Keeys, R.K., Heat transfer to steam-water-mixtures flowing in uniform heated tubes in which critical heat-flux has been exceede. Paper presented at Inst. Mechanical Eng. Convention, Bristol, 1968.

/5/ Adorni, N., Alia, P., Cravarolo, L., Hassid, A., An isokinetic sampling probe for phase and velocity distribution measurements in two-phase flow near the wall of condiut. CISE-Report 89, 1963.

/6/ Chisholm, D., Int. J. Heat and Mass Transfer 16, 347 ff. (1973).

/7/ Friedel, L., Improved friction pressure drop correlation for horizontal and vertical two-phase pipe flow. European Two-Phase Flow Meeting 7, Ispra, Italien, Paper E 2, 1979.

/8/ Ishii, M., Inception criteria for droplet entrainment in two-phase co-current film flow. AIChE J. 21 (2), 306 (1975).

/9/ Ueda, T., Nose, S., Studies of liquid film flow in two-phase annular and annular mist flow regimes. Bulletin of ISME 17, Nr. 107 (1974).

/10/ Levy, S., Prediction of two-phase flow with liquid entrainment. Int. J. Heat and Mass Transfer 9, 171 (1966).

/11/ Lopes, J.C.B., Dukler, A.E., Droplet sizes, dynamics and deposition in vertical annular flow. NUREG/CR-4424, 1985.

/12/ Asali, J.C., Leman, G.W., Handratty, T.J., Entrainment measurements and their use in design equations. PCH Vol.6, Nr.1/2, pp. 207-221, 1985.

/13/ Lopes, J.C.B., Dukler, A.E., Droplet entrainment in vertical annular flow and its contribution to momentum transfer. NUREG/CR-4729, R2, R4, 1986.

/14/ Wilson, J.F., The velocity of rising steam in a bubbling two phase mixture. ANS-Translation 5, 151 (1962).

/15/ Margulova T.H., An experimental investigation of the velocity in bubbling through a layer of water at high pressures. Trans. of the Power Inst. M.V. Molotow, Vol. 11, Moscow, 1953.

/16/ Behringer, P., Steiggeschwindigkeit von Dampfblasen in Kesselrohren. VDI-Forschungsheft 365.

/17/ Mersmann, A., Auslegung und Maßstanbsvergrößerung von Blasen und Tropfensäulen. Chem.-Ing.-Tech. 49, 679-770 (1977).

/18/ Sterman, L.S., The correlation of experimental data for vapour bubbling through a liquid. Zh. Tech. Fiz 26, 1519 (1956).

/19/ Kurbatov, A.V., The bubbling and the problem of critical loads in steam separators. Trans. of the Power Inst. M.V. Molotov, Vol. 11, Moscow, 1953.

/20/ Labuncov, D.A., Teploenergetica 7, 76-81 (1960).

/21/ Viecenz, H.-J., Blasenaufstieg und Phasenseparation in Behältern bei Dampfeinleitung und Druckentlastung. Dissertation, Technische Universität Hannover, 1980.

/22/ Zuber, N., Findlay, J.A., Average volumetric concentration in two-phase flow systems. Trans. ASME, J. Heat Transfer 87, 453-468 (1965).

/23/ Mandhane, J.M., Gregory, G.A., Aziz, K., A flow pattern map for gas-liquid flow in horizontal pipes. Int. J. Multiphase Flow 1, 537-553 (1974).

/24/ Taitel, Y., Dukler, A.E., A model for predicting flow regime transitions in horizontal and near horizontal gas-liquid flow. AIChE J. 22 (1), 47-55 (1976).

Wilson [6]	H_2O - H_2O vapour	d_{Vess} : 480 mm 100 mm sint. plate	$\langle\varepsilon\rangle = C\,[Fr]^a\,[We]^{0.1}\left[\frac{\rho_G}{\rho_L-\rho_G}\right]^{0.17}$	C = 0,68 a = 0,31 C = 0,88 a = 0,20	$\frac{w_{GO}}{[g\sqrt{\sigma/g(\rho_L-\rho_G)}]^{\frac{1}{4}}} < 2$ $\frac{w_{GO}}{[g\sqrt{\sigma/g(\rho_L-\rho_G)}]^{\frac{1}{4}}} > 2$	20 ÷ 41
Sterman Dementiev Lepilin [7]	H_2O H_2O vapour	d_{Vess} : 51 mm 69 mm 85 mm evaporator sint. plate	$\langle\varepsilon\rangle = C\,[Fr]^a\,[We]^{0.25}\left[\frac{\rho_G}{\rho_L-\rho_G}\right]^{0.17}$	C = 1,07 a = 0,40 C = 1,90 a = 0,17	$\frac{w_{GO}}{[g\sqrt{\sigma/g(\rho_L-\rho_G)}]^{\frac{1}{4}}} < 3.7$ $\frac{w_{GO}}{[g\sqrt{\sigma/g(\rho_L-\rho_G)}]^{\frac{1}{4}}} \geq 3.7$	1,07 ÷ 190
Margulova [8]	H_2O - H_2O vapour	d_{Vess}: 200 mm sint. plate	$\langle\varepsilon\rangle = (0{,}576 + 0{,}00414\,p\,[atm])\,w_{Go}^{0.75}$		no	91 ÷ 190
Kurbatov [9]	H_2O - H_2O vapour	d_{Vess}: 51 ÷ 200 mm evaporator sint. plate	$\langle\varepsilon\rangle = 0{,}67\,[Fr]^{\frac{1}{3}}\,[We]^{\frac{1}{6}}\left[\frac{\rho_L}{\rho_L-\rho_G}\right]^{\frac{1}{3}}\left[\frac{\nu_L}{\nu_G}\right]^{\frac{2}{3}}$		no	1,07 ÷ 190
Labuncov [10]		d_{Vess}: 17 ÷ 748 mm	$\langle\varepsilon\rangle = \left(1+\frac{w_{Bub}}{w_{Go}}\right)^{-1}$ $w_{Bub_\infty} = 1{,}5\left[\frac{g\,\sigma(\rho_L-\rho_G)}{\rho_L^2}\right]^{\frac{1}{4}}$ $\psi_L = 1{,}5\left(\frac{\rho_L}{\rho_G}\right)^{\frac{1}{3}}\left(1-\frac{\rho_G}{\rho_L}\right)^3$ $w_{Bub} = w_{Bub_\infty}\,\psi_L$		Bo > 500	1 ÷ 196
Mersmann [11]	air - H_2O H_2O - Hg Toluol-H_2O		$\langle\varepsilon\rangle(1-\langle\varepsilon\rangle)^n = 0.14\,w_{GO}\left(\frac{\rho_L^2}{g\,\sigma(\rho_L-\rho_G)}\right)^{\frac{1}{4}}$ $\left(\frac{\rho_L}{\rho_L-\rho_G}\right)^{\frac{1}{3}}\left[\frac{\sigma^3\rho_L^2}{\eta_L^4(\rho_L-\rho_G)g}\left(\frac{\rho_L}{\rho_G}\right)^{\frac{5}{3}}\right]^{\frac{1}{24}}$		$n = f\left(\frac{\rho_L}{\rho_G}\right)$	

Table 1: Empirical correlations for mean void fraction with phase separation

Tab. 2 : Constants and exponents in equation 14

	$\langle\bar{\varepsilon}\rangle < 0{,}104$	$C = 1{,}783$;	$a = -0{,}242$;	$b = 0{,}142$
$0{,}104 \leq$	$\langle\bar{\varepsilon}\rangle < 0{,}24$	$C = 2{,}20$;	$a = -0{,}143$;	$b = 0{,}147$
	$\langle\bar{\varepsilon}\rangle \geq 0{,}24$	$C = 1{,}0$;	$a = 0$;	$b = 0$